https://doi.org/10.1016/j.gaitpost.2021.03.005

Original article

Intrinsic foot muscle hardness is related to dynamic postural stability after landing in healthy young men

Noriaki Maeda[a,*], Arisu Hirota[a], Makoto Komiya[a], Masanori Morikawa[a], Rami Mizuta[a], Hironori Fujishita[b], Yuichi Nishikawa[c], Toshiki Kobayashi[d], Yukio Urabe[a]

[a]Division of Sport Rehabilitation, Graduate School of Biomedical and Health Sciences, Hiroshima University, 1-2-3 Kasumi, Minami-ku, Hiroshima 734-8553, Japan

[b]Sports Medical Center, Hiroshima University Hospital, 1-2-3 Kasumi, Minami-ku, Hiroshima 734-8551, Japan

[c]Faculty of Frontier Engineering, Institute of Science & Engineering, Kanazawa University, Kanazawa, Japan

[d]Department of Biomedical Engineering, Faculty of Engineering, The Hong Kong Polytechnic University, 11 Yuk Choi Road, Hung Hom, Hong Kong, China

***Corresponding author:**

Noriaki Maeda

1-2-3 Kasumi, Minami-ku, Hiroshima 734-8553, Japan

Tel.: +81 82-257-5410; Fax: +81 82-257-5344

E-mail: norimmi@hiroshima-u.ac.jp

Abstract

Background

The human foot has competent mechanisms for supporting weight and adapting movement to various surfaces; in particular, the toe flexor muscles aid in supporting the foot arches and may be important contributors to postural stability. However, the role of intrinsic foot muscle morphology and structure in the postural control system remains unclear, and the relationship between them is not well known.

Research question

Are intrinsic foot muscle morphology and toe flexor strength related to static and dynamic postural stability in healthy young men?

Methods

A total of 27 healthy men aged 19–27 years participated in this study. intrinsic foot muscle morphology included muscle hardness and thickness. Cross-sectional area was measured by ultrasonography at an ankle dorsiflexion angle of 0°. The hardness of the abductor hallucis (AbH), flexor hallucis brevis, and flexor digitorum brevis (FDB) muscles was measured using ultrasound real-time tissue elastography. Static postural stability during single-leg standing on a single force platform with closed eyes was assessed for the right leg. In the assessment of dynamic postural stability, the subjects jumped and landed on single-leg onto a force platform and the dynamic postural stability index (DPSI) was measured.

Results

FDB muscle thickness showed a positive correlation with anteroposterior stability index (APSI) ($r=0.398$, $p=0.040$). AbH muscle hardness was negatively correlated with APSI ($r=-0.407$, $p=0.035$); whereas FDB muscle hardness was positively correlated with DPSI ($r=0.534$, $p=0.004$), vertical stability index ($r=0.545$, $p=0.003$), and maximum vertical ground reaction force ($r=0.447$, $p=0.020$). Multiple regression with forced entry revealed that only DPSI was significantly correlated with FDB muscle hardness ($p=0.003$).

Significance

The results indicated that intrinsic foot muscle hardness plays an important role in dynamic postural control among healthy young men, which may enable a more rapid muscular response to changes in condition during jump landing and better performance in balance tasks.

Keywords

Muscle thickness; Cross-sectional area; Muscle hardness; Static postural stability; Dynamic postural stabil

1. Introduction

The human foot directly exposed to external forces from the ground has competent mechanisms for supporting weight and adapting movement to various surfaces [1]. In particular, the intrinsic muscles that aid in supporting the foot arches may play a role in the foot's flexibility for absorbing impact and its stiffness for transmitting force [2] and may be important contributors to postural stability [3,4]. Luke et al. [5] reported that intrinsic foot muscles (IFMs) in the human foot promote elastic energy storage and may modulate the energy storage capacity of the foot in addition to contributing to plantar aponeurosis. However, the role of intrinsic foot muscle morphology in the postural control system remains unclear. Postural control ability is an essential part of daily life and sport activities, and a postural stability deficit due to foot injury and deformity can lead to musculoskeletal disorders, including ankle sprains and falls [6].

Recent studies have pointed out that a decrease in the size and strength of IFM can reduce a person's ability to maintain balance during single-leg standing [7], as well as physical performance [8,9]. Identification of possible relationships between IFM morphology (muscle thickness, cross-sectional area [CSA], hardness) and postural control may reveal the factors associated with postural stability deficit resulting from abnormal IFM morphology and muscle weakness.

To the best of our knowledge, the relationship between IFM morphology and dynamic balance is not explored. Therefore, we hypothesized that IFM hardness was involved with the maintenance of dynamic postural stability among healthy young men with no abnormalities in foot structure or function. The present study aimed to investigate whether IFM morphology and toe flexor strength were related to static and dynamic postural stability after jump landing in healthy young men.

2. Methods

2.1. Subjects

A total of 27 healthy, recreationally active men (mean ± standard deviation [SD]: age, 21.9 ± 1.9 years; height, 171.6 ± 6.5 cm; body mass, 63.9 ± 2.3 kg) voluntarily participated in this study. “Recreationally active” was defined as participation in at least 150 min of moderate activity per week for at least 6 months according to the American College of Sports Medicine guidelines [10]. Subjects were not included in this study if they met any of the following non-inclusion criteria: (1) ligament injuries, plantar fasciitis, bursitis, and orthopedic injuries to the hip, knee, ankle, or foot; (2) a history of lower extremity trauma; and (3) neurological conditions that might affect balance ability. The average duration of each laboratory trial was 58.0 ± 2.0 min.

The study protocols complied with the principles laid down in the Declaration of Helsinki and were approved by the Ethical Committee for Epidemiology of Hiroshima University (approval number: E-2090). All subjects provided informed consent for their participation in the study.

2.2. Experimental procedure

2.2.1. Assessment using B-mode ultrasonography and real-time tissue elastography (RTE)

Images of IFM morphology (muscle thickness, CSA, and muscle hardness) were obtained with B-mode ultrasonography (HI VISION Avius; Hitachi Aloka Medical, Tokyo, Japan) and RTE using an 8-MHz linear array probe to visualize a continuous sagittal ultrasound image. An acoustic coupler (EZU-TECPL1; Hitachi Aloka Medical, Tokyo, Japan) was placed onto the transducer with a plastic attachment (EZU-TEATC1; Hitachi Aloka Medical, Tokyo, Japan) as reference material. The hardness value was calculated as 22.6 ± 2.2 kPa, which is a relative value based on the acoustic coupler in the material tests conducted by the manufacturer. A technician with 5 years of experience evaluated the ultrasound measurements.

2.2.2. Assessment of muscle thickness and CSA

Selected muscle thickness and CSA of the plumpest part of the muscle were measured with B-mode ultrasonography by following the same procedure used in previous studies [11,12] that measured the selected muscle in the contraction-free position by a linear array probe. The following were measured in the prone position, with the subjects' ankles in neutral position and their knees flexed at 90° to ensure the best contact of the probe with the skin while exerting minimal pressure on the tissue: (1) thickness of the abductor hallucis (AbH), flexor hallucis brevis (FHB), and flexor digitorum brevis (FDB); (2) CSA of the AbH, FHB, and FDB. The probe's position was marked on the skin surface with semi-permanent ink and was redrawn when it faded. The probe was placed along a line perpendicular to the long axis of the foot on the anterior aspect of the medial malleolus for the recording of CSA image of the AbH and was subsequently placed almost perpendicular to the same line for the recording of thickness image. Furthermore, the probe was placed perpendicular to a line parallel to the FHB muscle for the recording of CSA image of the FHB and was subsequently placed along the same line for the recording of thickness image. Additionally, the probe was placed along a line between the third toe and medial calcaneal tubercle for the recording of CSA image of the FDB and was subsequently placed along the same line for the recording of thickness image (Fig. 1).

Measurements of the thickness and CSA of IFM have been reported to be reliable in assessing plantar muscle thickness and CSA in previous protocols [13,14].

2.2.3. Assessment of muscle hardness using RTE

The scanning head of the probe was coated with transmission gel to achieve acoustic coupling. RTE images were obtained by manually applying light repetitive compression (rhythmic compression–relaxation cycle) with the transducer in the scan position. In order to obtain appropriate images for investigation, the examiner responsible for ultrasonography assessment pressed the transducer against the selected muscle with constant repeated pressure (the strain ratio in range of -0.7 to 0.7) and monitored the pressure indicator incorporated into the ultrasound scanner (Fig. 2). For each task, three images were randomly selected, and the average values were calculated after scanning. The hardness of the AbH, FHB, FDB were measured in the supine position, with the subjects' ankles in neutral position and their knees flexed at 90°; their thickness was measured in the same position as well. The RTE assessment took less than 10 min. RTE images were displayed as translucent, color-coded, real-time images superimposed on B-mode images, with red indicating a large distortion in response to the compression (the softest component), blue indicating least distortion (the hardest component), and green representing the mean strain. The mean strain in the region of interest (ROI) was monitored in a strain graph in order to adjust the force and frequency of the compression. When the elastogram was successfully superimposed on the ROI, the frequency was adjusted from 2 Hz to 4 Hz to maximize image quality. The strain rate within each ROI was automatically measured using built-in software, and the strain ratio (reference/muscle ratio; the strain measured in the reference ROI divided by the strain measured in the muscle ROI) was calculated for each image. The RTE in response to the compression force is physically smaller in harder tissue than in softer tissue; hence, as the muscles become stiffer, the RTE value becomes smaller [15]. RTE measurements were performed thrice, and the mean value within the ROI from these measurements was used in subsequent analyses. All measurements and positioning of all ROIs were performed by the same examiner. A high intra-observer reproducibility was previously reported for the reference/muscle ratio of RTE measurements (muscle/coupler) [16].

2.2.4. Single-leg standing test

The Single-leg standing test was carried out on a stabilometer (T.K.K. 5810; Takei Scientific Instruments Co. Ltd., Niigata Prefecture, Japan) as a first test in this study. The stabilometer was connected to a computer by an analog-to-digital converter (AI-

1608AY-USB; CONTEC, Osaka, Japan). Subjects were instructed to place both of their arms on the body trunk and to maintain an upright posture with their eyes closed and without the use of any support for 30 s. If the unsupported leg touched the force platform or weight-bearing foot, the trial was repeated. Statokinesigrams showing the entire range of postural sway from the central position on a chart were obtained; data were collected at a sampling frequency of 100 Hz. Subsequently, the locus length/second (mm/s) and enveloped area (mm^2) surrounded by the circumference of the wave pattern during single-leg standing were calculated. The locus length/second represents the total distance traveled by the center of pressure (COP) over time. This parameter is determined by dividing the total length by the trial duration. The enveloped area was defined as the area enclosed by the outermost path of the COP displacements.

2.2.5. Assessment of dynamic postural stability after landing

The dynamic postural stability index (DPSI) and maximum vertical ground reaction force (vGRFmax) were measured using a force plate (AccuGait; AMTI, Hiratsuka, Kanagawa, Japan) to obtain anterior-posterior, medial-lateral, and vertical ground reaction force. Dynamic postural stability after landing was evaluated using a 2-leg jump and 1-leg landing in the forward direction. In a previous study, this approach achieved an intersession reliability [ICC (3,k)] of 0.86 [17]. The jump height was standardized to 30 cm, whereas the jump distance was normalized to the subjects' body height [17]. The subjects placed 40% of their height from the end of the force plate, and a hurdle with a height of 30 cm was placed at the midpoint between the force plate and the starting position. The subjects performed the following actions 3 times: jumping in the forward direction using both of their legs over the hurdle with subsequent landing on the force plate using the non-dominant limb, stabilizing as quickly as possible, placing both of their hands on the waist once stabilized, and keeping still for 10 s while looking forward. In order to become familiar with the 1-leg jump, the subjects were permitted 5 practice trials for each condition, with 2 min of rest after testing. The task was repeated if the subjects fell upon landing, contacted the hurdle, or failed to jump. Three successful trials were performed and used for data analysis.

2.2.6. Toe flexor strength

Toe flexor strength was measured in the sitting position using a toe grip dynamometer (T.K.K.3361; Takei Scientific Instruments, Niigata, Japan), which consisted of strain gauge force transducers. Measurement of toe flexor strength involved a gradual increase in the toe flexor strength exerted by the toe flexor muscles for 0–3 s, with the maximum force held for 2 s. The force generated at the metatarsophalangeal joints was measured when the grip bar was pulled. The foot was placed on the dynamometer and was fixed with a heel stopper and belt. During measurement, the subjects were instructed to perform the task in the sitting position with their arms placed in front of their chest and with their hip and knee joints flexed at 90°. The average of 2 maximum force values for the toe flexor strength measured was used for further analysis.

2.3. Data collection

The locus length and enveloped area surrounded by the circumference of the wave pattern during postural sway in static postural control were calculated. Signals of static postural sway were recorded at a sampling frequency of 100 Hz via an analog-to-digital converter. Ground reaction force (GRF) data for DPSI calculation in dynamic postural control were also collected at a sampling frequency of 200 Hz. The GRF data were filtered using a zero-lag, fourth-order, low-pass Butterworth filter with a frequency cut-off of 20 Hz. From these filtered data, the DPSI was calculated using a Microsoft Excel Macro (Microsoft, Redmond, WA, USA). The dependent variable was the DPSI, as presented in Table 1.

The DPSI is a composite of anteroposterior, mediolateral, and vertical GRFs in all planes and is sensitive to force changes in mediolateral stability index (MLSI), anteroposterior stability index (APSI), and vertical stability index (VSI) directions. These are converted to APSI, MLSI, and VSI scores using the formula shown in Table 1 [18]. The DPSI was calculated using the GRFs generated within the first 3 s immediately after the initial contact, which was identified at the time when the vertical GRF exceeded 5% of the body weight. The force plate values were normalized to the body weight. $vGRF_{max}$ was calculated using raw data signals, and $vGRF_{max}$ normalized to the body weight of each subject was then used in the present study. The average of data from three successful trials for each condition was used for additional analysis [18].

2.4. Statistical analysis

Data were analyzed using EZR (Saitama Medical Center, Jichi Medical University, Saitama, Japan) [19]. Shapiro–Wilk test was conducted to test normality. Normally and non-normally distributed variables are presented as mean ± SD and as median and interquartile range (IQR), respectively. Normally and non-normally distributed variables are presented as mean ± SD and as median and interquartile range (IQR), respectively. Prior to analysis, the normal distribution of data was confirmed using the Shapiro–Wilk test. Correlation coefficients were calculated using a Spearman's rank correlation test to detect the possible relationships of the thickness, CSA, and RTE of the assessed muscles with static and dynamic balance stability results. A p-value of <0.05 was considered to indicate statistical significance.

Multiple linear regression with forced entry was performed to examine the association of IFM thickness, CSA, and RTE with the DPSI, which was used as a dynamic balance index. To avoid overfitting due to the small sample size, we used each value for IFM morphology independently.

As referred to in the previous report [20], a post hoc power analysis was conducted. The analysis procedure required the population "Effect size f^2," the "α err prob," the "Total sample size," and the "Number of predictors" in the regression model as input parameters to obtain the power of the omnibus *F* test ("Power [1 err prob]").

3. Results

The mean, median, IQR, and SD values of ultrasonographic evaluations, balance assessments, and toe flexor strength measurement are presented in Table 2. Correlation analysis revealed that a larger FDB was associated with a reduced performance in dynamic balance stability in Table 3. FDB thickness was positively correlated with APSI (r=0.398, p=0.040). Additionally, the RTE of the AbH was negatively correlated with

APSI ($r=-0.407$, $p= 0.035$), whereas the RTE of the FHB was positively correlated with DPSI ($r=0.534$, $p=0.040$), VSI ($r=0.545$, $p= 0.003$), and $vGRF_{max}$ ($r=0.447$, $p= 0.020$). Table 4 summarizes the results of multiple regression analysis for the association between IFM morphology characteristics assessed by ultrasonography and the DPSI values. Data were adjusted for logarithmically transformed (_L) age, BMI_L, postoperative time_L, and sex. Thickness and CSA were not associated with the DPSI. Only the RTE was associated with the DPSI. As shown in the results of the post hoc power analysis, the model of multiple regression analysis for the association between RTE and DPSI had sufficient power ($1-\beta$ err prob = 0.86).

4. Discussion

The main finding of the present study indicated that the single-leg standing test for static postural stability was not associated with IFM morphology. Only the DPSI, a measure of dynamic balance, was associated with FDB hardness.

The foot has spring-like properties, storing and releasing elastic energy with each foot strike. This is accomplished by the deformation of the arch, which is controlled by the intrinsic and extrinsic muscles of the foot. Especially, IFM have the ability to maintain foot arches and adapt to the velocity during standing and walking [21]. Therefore, when plantar muscle weakness or deformity occurs, the foot arches also collapse, which may reduce a person's ability to adapt to movement and, hence, static and dynamic balance ability [3].

Tas et al. [12] reported that smaller thickness and CSA of the AbH, FHB, and FDB were associated with a better performance in static balance tasks, whereas higher stiffness of the AbH and FHB was correlated with a better performance in single-leg stance balance assessments among healthy sedentary young females. In contrast, Zhang et al. [11] reported that the thickness and CSA of the FDB did not affect the performance of recreational runners in balance tasks during single-leg standing. The present study did not show a significant correlation between the morphological features of FDB and static balance ability, similar to the results reported by Zhang et al. [11].

To the best of our knowledge, this is the first study that investigated the relationship between AbH and FDB muscle hardness and dynamic balance ability. Previous study has reported that the muscle activity of the AbH and FDB muscles increases as the required static balance ability increases [22]. These results suggested the AbH and FDB muscles are related to postural control as shown in the present study. Furthermore, the relationship between IFM stiffness and performance in balance tasks may be associated with the sensorimotor interactions between these muscles and plantar muscles, which contribute to the aggregation of sensory information related to postural control [21,23].

The results indicated that AbH and FDB hardness is associated with dynamic balance ability. The relationship between IFM hardness and performance in balance tasks can provide relevant sensory information about foot posture and directly support muscle contraction to control posture.

The association between IFM morphology and balance ability demonstrated in this study has been shown in previous studies. High plantar intrinsic muscle stiffness may improve the performance in tasks requiring the sense of balance via improvement in kinetic sensation due to the increased sensitivity of muscle spindles [24]. According to Tas et al. [12] showed that higher FDB hardness might contribute to the stabilization of dynamic balance after landing as well as better performance in dynamic balance tasks. In a previous study of the response time of IFM to electrical stimulation, FDB was characterized by a significantly faster response time [25]. In addition, afferent signals from sensory receptors in the ankle joint are associated with reflexive muscle activity of FDB [26]. In other words, hardness of FDB may have increased the sensitivity of the muscle spindles, resulting in a faster reaction time of muscle activity to postural sway and, consequently, a higher dynamic balance after landing.

The present study has a few limitations that need to be considered. In this study, only healthy young men without abnormal feet were included. IFM morphologies may differ among different populations, such as children, women, and elderly persons. Moreover, subjects with foot deformities such as hallux valgus or flatfoot were not included. Further studies investigating differences in IFM morphology and balance ability among subjects with these foot deformities are needed.

From the standpoint of clinical daily practice, the results in this study could be applied to improve prognoses and quality of treatments for patients with foot deformities, such as pes planus.

In conclusion, IFM hardness plays an important role in dynamic postural control among healthy young men.

Acknowledgements

We would like to thank all volunteers for their participation in this study, as well as Editage (http://www.editage.jp/) for English language editing.

Declarations of interest

None.

Funding

This research did not receive any specific grant from funding agencies in the public, commercial, or not-for-profit sectors.

CRediT authorship contribution statement

Noriaki Maeda, Toshiki Kobayashi: Investigation, Resources, Writing - original draft, Writing - review & editing. **Arisu Hirota, Makoto Komiya, Masanori Morikawa:** Software, Visualization. **Toshiki Kobayashi:** Methodology. **Arisu Hirota, Hironori Fujishita, Yuichi Nishikawa, Yukio Urabe:** Formal analysis. **Rami Mizuta, Yukio Urabe:** Data curation.

References

[1] L. Welte, L.A. Kelly, G.A. Lichtwark, M.J. Rainbow, Influence of the windlass mechanism on arch-spring mechanics during dynamic foot arch deformation, J. R. Soc. Interface. 15 (2018) 20180270. https://doi.org/10.1098/rsif.2018.0270.

[2] U.T. Taddei, A.B. Matias, F.I.A. Ribeiro, S.A. Bus, I.C.N. Sacco, Effects of a foot strengthening program on foot muscle morphology and running mechanics: A proof-of-

concept, single-blind randomized controlled trial, Phys. Ther. Sport. 42 (2020) 107–115. https://doi.org/10.1016/j.ptsp.2020.01.007.

[3] E.P. Mulligan, P.G. Cook, Effect of plantar intrinsic muscle training on medial longitudinal arch morphology and dynamic function, Man. Ther. 18 (2013) 425–430. https://doi.org/10.1016/j.math.2013.02.007.

[4] J.W. Wallace, B.G. Rasman, B.H. Dalton, Vestibular-evoked responses indicate a functional role for intrinsic foot muscles during standing balance, Neuroscience. 377 (2018) 150–160. https://doi.org/10.1016/j.neuroscience.2018.02.036.

[5] L.A. Kelly, D.J. Farris, A.G. Cresswell, G.A. Lichtwark, Intrinsic foot muscles contribute to elastic energy storage and return in the human foot. 126 (2019) 231–238. https://doi.org/10.1152/japplphysiol.00736.2018

[6] A. Merlo, D. Zemp, E. Zanda, S. Rocchi, F. Meroni, M. Tettamanti, et al., Postural stability and history of falls in cognitively able older adults: The Canton Ticino study, Gait Posture. 36 (2012) 662–666. https://doi.org/10.1016/j.gaitpost.2012.06.016.

[7] Y. Suponitsky, O. Verbitsky, E. Peled, J. Mizrahi, Effect of selective fatiguing of the shank muscles on single-leg-standing sway, J. Electromyogr. Kinesiol. 18 (2008) 682–689. https://doi.org/10.1016/j.jelekin.2007.01.009.

[8] S.K. Lynn, R.A. Padilla, K.K.W. Tsang, Differences in static- and dynamic-balance

task performance after 4 weeks of intrinsic-foot-muscle training: the short-foot exercise versus the towel-curl exercise, J. Sport Rehabil. 21 (2012) 327–333. https://doi.org/10.1123/jsr.21.4.327.

[9] J.P. Goldmann, M. Sanno, S. Willwacher, K. Heinrich, G.P. Bruggemann, The potential of toe flexor muscles to enhance performance, J. Sports Sci. 31 (2013) 424–433. https://doi.org/10.1080/02640414.2012.736627.

[10] L.S. Pescatello, American College of Sports Medicine, ACSM's Guidelines for Exercise Testing and Prescription, ninth ed., Wolters Kluwer/Lippincott Williams & Wilkins Health, Philadelphia, 2014.

[11] X.Y. Zhang, K.H. Schutte, B. Vanwanseele, Foot muscle morphology is related to center of pressure sway and control mechanisms during single-leg standing, Gait Posture. 57 (2017) 52–56. https://doi.org/10.1016/j.gaitpost.2017.05.027.

[12] S. Tas, N.O. Unluer, A. Cetin, Thickness, cross-sectional area, and stiffness of intrinsic foot muscles affect performance in single-leg stance balance tests in healthy sedentary young females, J. Biomech. 99 (2020) 109530. https://doi.org/10.1016/j.jbiomech.2019.109530.

[13] G. Crofts, S. Angin, K.J. Mickle, S. Hill, C.J. Nester, Reliability of ultrasound for measurement of selected foot structures, Gait Posture. 39 (2014) 35–39. https://doi.org/

10.1016/j.gaitpost.2013.05.022.

[14] S. Angin, K.J. Mickle, C.J. Nester, Contributions of foot muscles and plantar fascia morphology to foot posture, Gait Posture. 61 (2018) 238–242. https://doi.org/10.1016/j.gaitpost.2018.01.022.

[15] O. Yanagisawa, J. Sakuma, Y. Kawakami, K. Suzuki, T. Fukubayashi, Effect of exercise-induced muscle damage on muscle hardness evaluated by ultrasound real-time tissue elastography, Springerplus. 4 (2015) 308. https://doi.org/10.1186/s40064-015-1094-4.

[16] O. Yanagisawa, M. Niitsu, T. Kurihara, T. Fukubayashi, Evaluation of human muscle hardness after dynamic exercise with ultrasound real-time tissue elastography: A feasibility study, Clin. Radiol. 66 (2011) 815–819. https://doi.org/10.1016/j.crad.2011.03.012.

[17] E.A. Wikstrom, M.D. Tillman, A.N. Smith, P.A. Borsa, A new force-plate technology measure of dynamic postural stability: The dynamic postural stability index, J. Athl. Train. 40 (2005) 305–309.

[18] E.A. Wikstrom, M.A. Arrigenna, M.D. Tillman, P.A. Borsa, Dynamic postural stability in subjects with braced, functionally unstable ankles, J. Athl. Train. 41 (2006) 245–250.

[19] Y. Kanda, Investigation of the freely available easy-to-use software 'EZR' for medical statistics, Bone Marrow Transplant. 48 (2013) 452–458. https://doi.org/10.1038/bmt.2012.244.

[20] F. Faul, E. Erdfelder, A. Buchner, A.G. Lang, Statistical power analyses using G*Power 3.1: tests for correlation and regression analyses, Behav. Res. Methods. 41 (2009) 1149–1160. https://doi.org/10.3758/BRM.41.4.1149.

[21] P.O. McKeon, J. Hertel, D. Bramble, I. Davis, The foot core system: a new paradigm for understanding intrinsic foot muscle function, Br. J. Sports Med. 49 (2015) 277. https://doi.org/10.1136/bjsports-2014-094485.

[22] L. A. Kelly, S. Kuitunen, S. Racinais, A. G. Cresswell: Recruitment of the plantar intrinsic foot muscles with increasing postural demand, Clinical Biomechanics. 27 (2012) 46-51. https://doi:10.1016/j.clinbiomech.2011.07.013

[23] E. Ferrari, G. Cooper, N.D. Reeves, E.F. Hodson-Tole, Intrinsic foot muscles act to stabilise the foot when greater fluctuations in centre of pressure movement result from increased postural balance challenge, Gait Posture. 79 (2020) 229–233. https://doi.org/10.1016/j.gaitpost.2020.03.011.

[24] V.G. Macefield, T.P. Knellwolf, Functional properties of human muscle spindles, J. Neurophysiol. 120 (2018) 452–467. https://doi.org/10.1152/jn.00071.2018.

[25] D. Tosovic, E. Ghebremedhin, C. Glen, M. Gorelick, JM. Brown, The architecture and contraction time of intrinsic foot muscles. J Electromyogr Kinesiol 22 (2012) 930–938, 2012. https://doi.org/10.1016/j.jelekin.2012.05.002 .

[26] M. Sakita, Y. Ishii, S. Takasugi, T. Saito, S. Kumagai, Effects of short and medium latency reflexes of the plantae. J Phys Ther Sci 24 (2012) 83–87. https://doi.org/10.1589/jpts.24.83.

Table 1. Equations for calculation of APSI, MLSI, VSI and DPSI

Variable	Equation
APSI	$= \sqrt{\dfrac{\Sigma(0 - \mathrm{GRFx})^2}{\text{Number of data point}}} \div \text{Body Weight}$
MLSI	$= \sqrt{\dfrac{\Sigma(0 - \mathrm{GRFy})^2}{\text{Number of data point}}} \div \text{Body Weight}$
VSI	$= \sqrt{\dfrac{\Sigma(0 - \mathrm{GRFz})^2}{\text{Number of data point}}} \div \text{Body Weight}$
DPSI	$= \sqrt{\dfrac{\Sigma(0 - \mathrm{GRFx})^2 + \Sigma(0 - \mathrm{GRFy})^2 + \Sigma(\text{Body Weight} - \mathrm{GRFz})^2}{\text{Number of data point}}} \div \text{Body Weight}$

DPSI : Dynamic Postural Stability Index ; MLSI: Medial-lateral stability index ; APSI : Anterior-posterior stability index ;
VSI : Vertical stability index ; GRF : Ground Reaction Force

The DPSI is a composite of the anterior-posterior, medial-lateral, and vertical ground reaction forces, and also provides stability indices for the anterior-posterior (APSI), medial-lateral (MLSI), and vertical (VSI) directions.

The DPSI was calculated using the ground reaction forces generated in the first three seconds immediately following initial contact that was identified as the instant when the vertical ground reaction force exceeded 5% of the body weight. The force plate data were normalized to body weight.

Table 2. Medial (interquartile range) and mean (standard deviation) values of assessed parameters.

Parameters	Median (interquartile range)				Mean (standard deviation)
Age (years)	22.0	(	21.0- 23.0	)	21.9 ± 1.9
Height (m)	171.0	(	167.5- 174.5	)	171.6 ± 6.5
Weight (kg)	64.0	(	59.5- 67.5	)	63.9 ± 6.1
BMI (kg/m2)	21.6	(	20.4- 23.2	)	21.7 ± 2.3
FPI	2.0	(	1.0- 3.5	)	2.4 ± 1.9
Thickness of selected tissues (mm)					
Abductor hallucis	12.0	(	10.4- 13.6	)	276.4 ± 62.2
Flexor hallucis brevis	12.8	(	12.2- 13.6	)	12.8 ± 1.5
Flexor digitorum brevis	9.9	(	7.8- 11.1	)	9.5 ± 2.4
Cross-sectional area of selected tissues (mm^2)					
Abductor hallucis	266.0	(	247.0- 309.1	)	276.4 ± 62.2
Flexor hallucis brevis	261.5	(	229.9- 274.9	)	256.5 ± 33.7
Flexor digitorum brevis	225.1	(	199.4- 254.7	)	227.6 ± 45.0
Ultrasound elastgraphy of selected tissues (muscle/coupler)					
Abductor hallucis	0.67	(	0.50- 0.94	)	0.9 ± 0.6
Flexor hallucis brevis	1.48	(	1.24- 2.21	)	1.8 ± 0.8
Flexor digitorum brevis	2.57	(	1.60- 3.90	)	2.8 ± 1.4
Single-leg standing test					
Mean velocity of COP (mm/s)	85.7	(	77.9- 97.3	)	85.4 ± 16.7
Sway area of COP (mm^2)	1788.8	(	1495.1- 2137.3	)	1829.5 ± 470.0
Rectangle area of COP (mm2)	2871.2	(	2335.9- 3220.3	)	2837.7 ± 715.0
Dynamic postural stablity index					
DPSI	0.304	(	0.290- 0.333	)	0.310 ± 0.304
MLSI	0.029	(	0.027- 0.035	)	0.03 ± 0.01

APSI	0.137	(0.127 - 0.147)	0.137 ± 0.013
VSI	0.267	(0.254 - 0.299)	0.275 ± 0.037
vGRF max (%BW)	2.8	(2.6 - 3.1)	2.8 ± 0.4
Toe flexor muscle strength (kg)	24.4	(20.0 - 29.1)	24.3 ± 6.5

Abbreviation: BMI, body mass index; FPI, COP; center of pressure, foot posture index; DPSI, dynamic postural stability index; MLSI, medial lateral stability index; APSI, anterior posterior stabiltiy index; VSI, vertical stability index; vGRF max, maximum vertical grand reaction force

Table 3. Correlation analysis between ultrasonographic measurements and balance assessment.

	Mean velocity of COP (mm/s)	Sway area of COP (mm^2)	Rectangle area of COP (mm^2)	DPSI		MLSI		APSI		VSI		vGRF max	
				r	p	r	p	r	p	r	p	r	p
Thickness of selected tissues (mm)													
Abductor hallucis[a]	-0.143	-0.196	-0.231	0.125	0.533	-0.323	0.101	0.059	0.770	0.124	0.536	0.071	0.725
Flexor hallucis brevis[a]	-0.164	-0.143	-0.089	0.067	0.739	0.130	0.518	0.125	0.534	0.048	0.810	0.172	0.391
Flexor digitorum brevis[a]	-0.044	-0.156	-0.152	-0.304	0.123	0.041	0.840	0.398*	0.040	-0.237	0.234	-0.071	0.724
Cross-sectional area of selected tissues (cm^2)													
Abductor hallucis[a]	-0.139	-0.118	-0.082	-0.244	0.219	0.054	0.790	-0.038	0.853	-0.249	0.211	-0.047	0.815
Flexor hallucis brevis[a]	-0.294	-0.201	-0.132	-0.115	0.569	-0.028	0.891	0.196	0.328	-0.151	0.452	-0.046	0.820
Flexor digitorum brevis[a]	-0.147	-0.218	-0.223	0.119	0.554	-0.099	0.622	-0.192	0.338	0.166	0.409	0.242	0.225
Ultrasound elastgraphy of selected tissues (muscle/coupler)													
Abductor hallucis[b]	-0.009	0.124	0.061	-0.215	0.282	-0.203	0.310	-0.407*	0.035	-0.152	0.450	-0.062	0.759
Flexor hallucis brevis[a]	0.078	0.121	0.161	0.067	0.739	0.065	0.748	-0.065	0.748	0.017	0.933	-0.130	0.518
Flexor digitorum brevis[a]	0.296	0.297	0.292	0.534**	0.004	0.137	0.496	0.025	0.903	0.545**	0.003	0.447**	0.020

*$p<0.05$, **$p<0.01$.

[a]Each variable was tested by the Pearson correlation coefficient.

[b]Each variable was tested by the Spearman's rank correlation coefficient.

Abbreviation: COP; center of pressure, DPSI, dynamic postural stability index; MLSI, medial lateral stability index; APSI, anterior posterior stabiltiy index; VSI, vertical stability index; vGRF max, maximum vertical grand reaction force

Table 4. Multiple regression analysis of associations of ultrasound elastgraphy of selected tissues with single-leg standing test and dynamic postural stability index

Ultrasound elastgraphy of selected tissues (muscle/coupler)	Single-leg standing test (COP velocity)				Dynamic postural stability index (DPSI)			
	β	95% CI interval		P	β	95% CI interval		P
		Lower	Upper			Lower	Upper	
Abductor hallucis	-0.21	-17.93	6.96	0.369	-0.29	-0.04	0.01	0.138
Flexor hallucis brevis	-0.04	-11.64	9.72	0.853	-0.07	-0.02	0.01	0.706
Flexor digitorum brevis	0.33	-1.39	9.45	0.136	0.58	0.01	0.02	**0.003**

Explanatory variables were ultrasound elastgraphy of abductor hallucis, flexor hallucis brevis, flexor digitorum brevis,.

β : standardised partial regression coefficient, CI: confidential interval, COP: center of pressure: DPSI, dynamic postural stability index.

Probe positions

(a) (b)

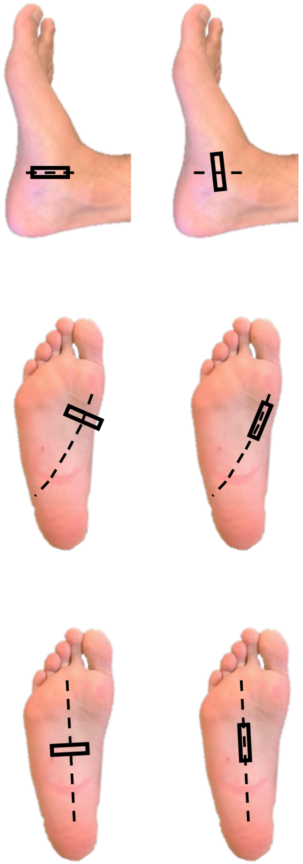

Definitions

Abductor hallucis(AbH)

Probe was placed along a line perpendicular to the long axis of the foot on the anterior aspect of the medial malleolus (a) for the recording of CSA, then subsequently placed almost perpendicular to the same line (b) for the recording of thickness image.

Flexor hallucis brevis(FHB)

Probe was placed perpendicular to a line parallel to the FHB muscle (a) for the recording of CSA, then subsequently placed along the same line (b) for the recording of thickness image.

Flexor digitorum brevis(FDB)

Probe was placed along a line between the third toe and medial calcaneal tubercle (a) for the recording of CSA, then subsequently placed along the same line (b) for the recording of thickness image.

Figure 1. The probe's position of assessment of muscle thickness and CSA

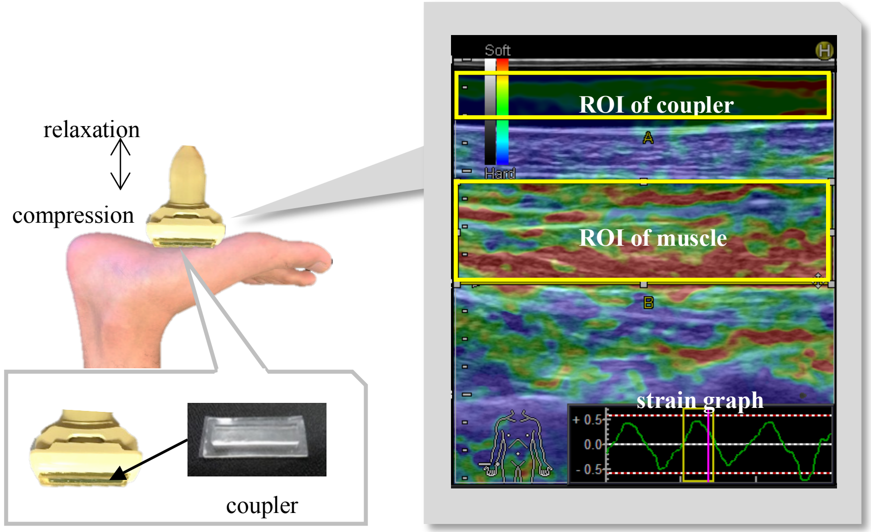

Figure 2. Assessment of muscle hardness using RTE and RTE images

We pressed the transducer against the selected muscle with constant repeated pressure (compression-relaxation cycle) by checking strain graph. Then, we selected ROI of coupler and muscle, and strain ratio (muscle/coupler) was calculated.